Influence of Hold Times on Fatigue Life and Fracture Behavior of Cast Superalloy INCONEL 713LC at 700°C

K. Obrtlík[1], J. Man[1], M. Petrenec[1], J. Polák[1], T. Podrábský[2]
[1]*Institute of Physics of Materials, Academy of Sciences of the Czech Republic, Brno, Czech Republic;* [2]*Brno University of Technology, Faculty of Mechanical Engineering, Brno, Czech Republic*

Abstract

The influence of tensile strain holds on fatigue life and fracture behavior in cast nickel-based superalloy INCONEL 713 LC was studied under symmetrical total strain cycling at 700 °C in air.

The microstructure of the superalloy is documented. Continuous cycling and cycling with 10 min dwell in the tensile tip of the hysteresis loop were applied to cylindrical specimens. Surface topography, fracture surface and specimen sections were observed in SEM.

Fatigue life in Manson-Coffin and Basquin representation in cycling with dwells is reduced in comparison with continuous cycling. Pure fatigue and pure creep data are used to analyze the fatigue damage with dwells. Surface relief and fracture surface observations reveal the change in damage mechanisms with the introduction of dwells. Density of slip markings in cycling with dwells decreases in comparison with continuous cycling. The life reduction due to dwells is discussed with respect to fatigue interaction with creep and environment.

1. Introduction

INCONEL 713 (IN 713) and its low carbon variant IN 713LC are widely used in many applications of power generation industry (e.g. for turbocharger wheels and gas turbine integral wheels). In service, the critical components are subjected to complex stress conditions. Considerable straining results mainly from temperature gradients during start-up and shut-down procedures or thermal transients. The in-service conditions can be approximated by strain controlled low cycle fatigue (LCF) tests with the introduction of dwells that simulate time-dependent effects during steady-state operation [1-3].

Effects of hold-time on LCF lifetime in a number of materials including superalloys are reviewed by Goswami [4]. Nickel-based superalloys are mostly dwell sensitive, i.e. the introduction of a dwell in the fatigue cycle results in a fatigue life reduction in comparison with continuous cycling. However, dwell cycles are beneficial to the fatigue life in isolated cases [4]. High temperature LCF and high cycle fatigue (HCF) data are reported only for isothermal continuous cycling in IN 713 and IN 713LC [5-8].

Hold-time effects in LCF include fatigue and creep damage and the damage due to fatigue-creep-environment interactions. Several attempts have been used to assess the component life under high temperature fatigue–creep conditions but the corrosion effects are not well understood [3,9-11]. Poor corrosion resistance of some cast alloys including IN 713LC suggests that environmental interactions are of particular importance [2]. The aim of the present contribution is to report the results of the study of tensile strain hold effects on the fatigue life and fracture behavior in cast polycrystalline nickel base superalloy IN 713 LC under symmetrical total strain cycling at 700 °C in air. Fatigue and creep damage accumulation are evaluated.

2. Experimental details

IN 713LC polycrystals were supplied by PBS Velká Bíteš, a.s. as conventionally cast rods. Chemical composition is shown in Table 1. Polished sections of the material reveal coarse grains with dendrites, carbides and shrinkage pores. The maximum shrinkage pore observed was 0.4 mm in diameter. The mean grain size, found using the linear intercept method, was 3.5 mm. The coarse grains imply that only several grains are present in the specimen gauge length. Therefore, significant scatter of elastic modulus measured on individual specimens was found. Typical values were in the interval from 141 to 183 GPa at 700 °C.

Fatigue tests were performed on cylindrical button-end specimens having gauge length and diameter of 15 and 6 mm, respectively [12]. Specimens were machined parallel to the rod axis and their gauge length was mechanically ground. The gauge section of some specimens was mechanically and electrolytically polished in order to facilitate the surface relief observation.

Table 1. Chemical composition of IN 713LC (in wt. %).

Cr	Al	Mo	Nb	Ti	Ta	Fe	Zr	Co
11.86	5.77	4.68	1.99	0.81	0.16	0.10	0.09	<0.05

C	B	Mn	Si	Cu	P	S	Ni
0.04	0.012	<0.05	<0.05	<0.05	0.007	0.005	Bal.

The specimens were fatigued in a computer controlled electrohydraulic testing system under strain control with fully reversed total strain cycle (R_ε = -1). The strain was measured and controlled using sensitive extensometer with a 12 mm base. The strain rate of $2x10^{-3}$ s^{-1} and total strain amplitude were kept constant in each test. The tests were conducted at 700 °C in air. Heating was provided by a three-zone resistance furnace and monitored by three thermocouples attached to both specimen ends and to one end of the gauge section. Two types of tests were applied. Continuous cycling and cyclic loading with 10 min dwell at the tensile peak strain in each cycle. Corresponding waveforms and hysteresis loops are shown in Fig. 1. $\Delta\sigma_r$ is the stress relaxed during the hold time. If unloading is elastic with Young's modulus E then the increase in plastic strain range due to relaxation $\Delta\varepsilon_{pr}$ can be obtained from

$$\Delta\varepsilon_{pr} = \Delta\sigma_r/E. \quad (1)$$

Hysteresis loops for selected numbers of cycles were recorded. Plastic strain amplitude ε_{ap} derived from the half of the loop width and stress amplitude σ_a at

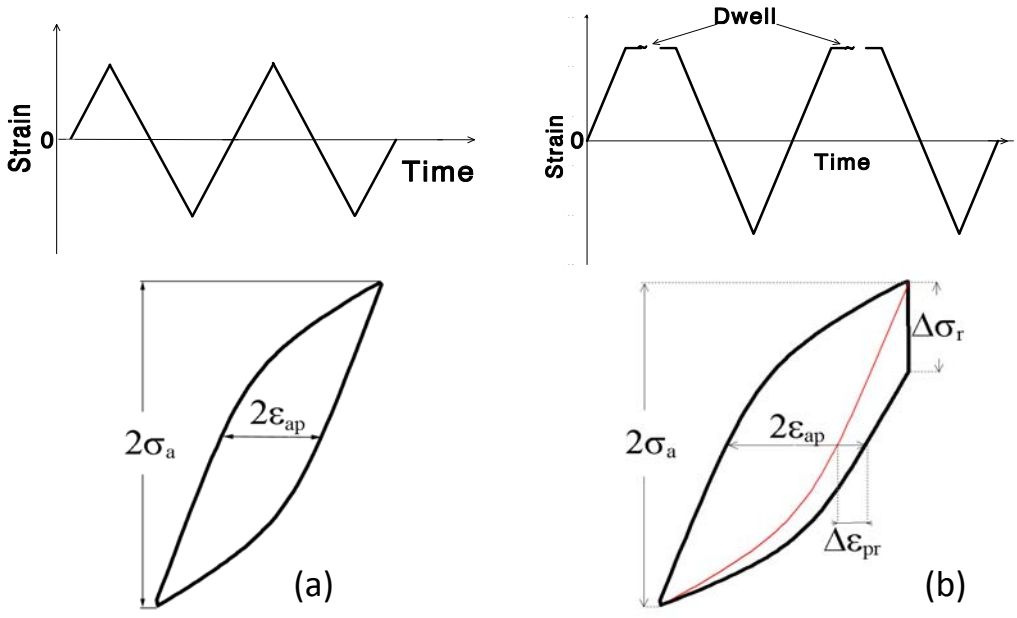

Fig. 1. Schematic diagram of waveforms and hysteresis loops in (a) continuous cycling (b) cycling with dwells.

half-life were evaluated.

Surface relief of the gauge area, gauge sections parallel to the specimen axis and fracture surfaces were observed in Philips 505 SEM on selected specimens cycled to fracture.

3. Results and discussion

3.1 Fatigue life

Fatigue life curves are plotted in Figs 2-4 for both continuous cycling and cycling with 10 min dwells. Fig. 2 shows the total strain amplitude vs. the number of cycles to failure. It can be seen that IN 713LC is tensile dwell sensitive. Introduction of dwell periods results in fatigue life reduction. The reduction is more pronounced at the lowest strain amplitudes (factor 9) than at the highest strain amplitudes (factor 3).

Figure 3 shows the fatigue life curves in the representation of plastic strain amplitude at half life ε_{ap} vs. number of cycles to failure N_f. Experimental data were approximated by the Manson-Coffin law

$$\varepsilon_{ap}=\varepsilon_f^{'}(2N_f)^c \qquad (2)$$

and the fatigue ductility coefficient $\varepsilon_f^{'}$ and the fatigue ductility exponent c were evaluated using regression analysis: $\varepsilon_f^{'} = 0.070 \pm 0.28$ (0.15 ± 0.22) and $c = -0.84 \pm 0.05$ (-1.10 ± 0.23) for continuous cycling (for cycling with dwells). Figure 3 shows that the Manson-Coffin curve is dwell dependent. Experimental data for the test with dwells are shifted to lower fatigue lives in comparison with

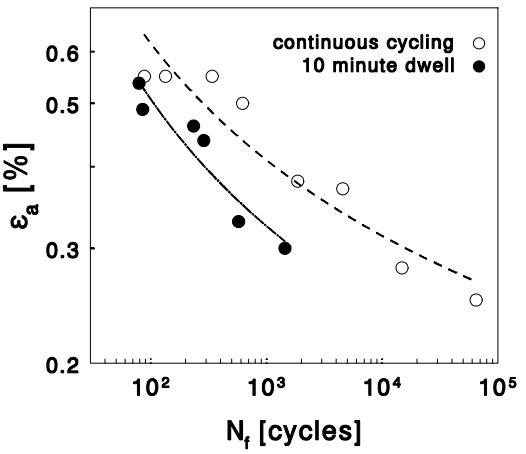

Fig. 2. Total strain amplitude vs. number of cycles to fracture.

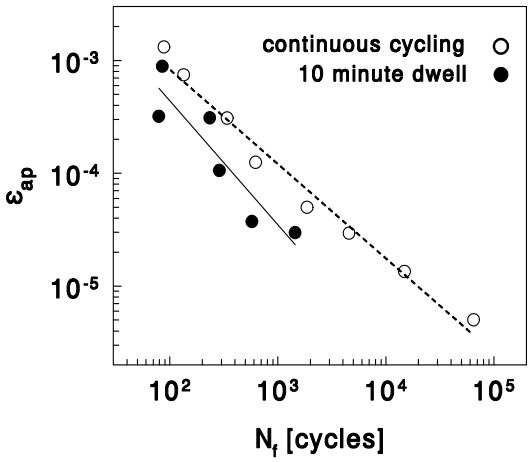

Fig. 3. Manson-Coffin plot for IN 713LC.

continuous cycling data. Moreover, the fatigue ductility exponent in the Manson-Coffin law decreased with hold-time from -0.84 to -1.1. This behaviour indicates that the dwell effect cannot be explained by the increase in plastic strain amplitude alone. Additional damage due to the fatigue-creep-environment interaction has to be taken into account.

Fatigue life curves in the representation of stress amplitude σ_a at half life vs. number of cycles to fracture N_f are shown in Fig. 4. Experimental data were fitted by the Basquin law:

$$\sigma_f = \sigma_f'(2N_f)^b \tag{3}$$

and the fatigue strength coefficient σ_f' and the fatigue strength exponent b were evaluated using regression analysis: σ_f' = (1610 ± 110) MPa {(1530 ± 410) MPa} and b = -0.12 ± 0.01 {-0.13 ± 0.04} for continuous cycling {for cycling with dwells}. The Basquin curve is sensitive to dwells as well. For the given stress amplitude the number of cycles to fracture decreases with the introduction of tensile dwells.

3.2 Fatigue-creep-environment damage

Damage accumulation in the course of the strain controlled fatigue tests with tensile dwells is analyzed with the generalized damage accumulation rule [11]

$$N_f(\varepsilon_{apef}) / n_f(\varepsilon_{apef}) + \sum_n \sum_i (t_{ni+1} - t_{ni}) / t_r((\sigma_{ni+1} + \sigma_{ni})/2) + D(tdi) = 1 \tag{4}$$

combining Palmgren-Miner damage rule and creep life fraction damage rule. D(tdi) is the damage due to time-dependent-interaction processes. N_f is the number of cycles to fracture of individual specimens in the test with hold-times, $\varepsilon_{apef} = (4\varepsilon_{ap} - \Delta\varepsilon_{pr})/4$ is an effective cyclic plastic strain amplitude in the test with

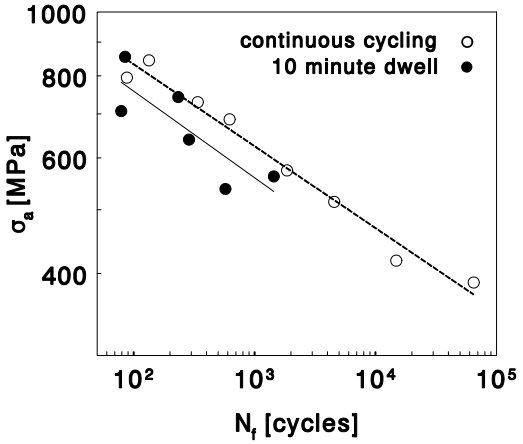

Fig. 4. Basquin curves of IN 713LC.

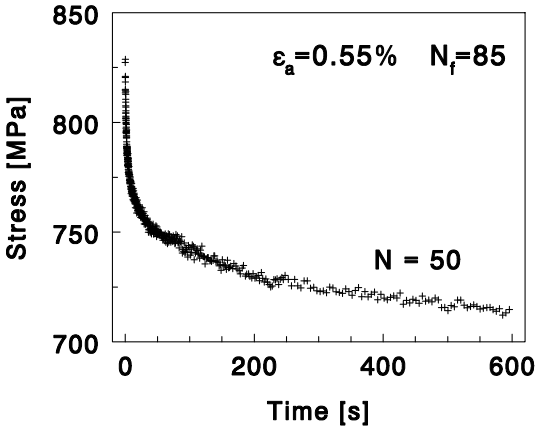

Fig. 5. Time dependence of stress relaxation.

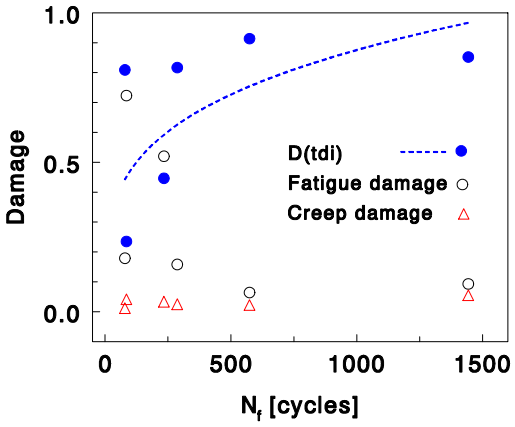

Fig. 6. Fatigue, creep and fatigue-creep-environment interaction damage vs. number of cycles to fracture for tests with dwells.

hold-times where ε_{ap} is derived from the hysteresis loop width and $\Delta\varepsilon_{pr}$ is obtained from Eq.1 (see Fig. 1). n_f is calculated from the Manson-Coffin curve (Eq. 2) of the continuous cycling test. Plastic strain amplitude instead of total strain amplitude is used in the Palmgren-Miner damage rule because Young's modulus E of individual specimens differs.

The creep life fraction, given by the second term in Eq. 4, represents creep damage and it is obtained using stress relaxation curves measured in the present work and the time-temperature parameter P_{LM} of Larson and Miller determined for IN 713LC elsewhere [13]. An example of the stress relaxation curve is shown in Fig. 5 for the 50th cycle in a test with strain amplitude of 5.5x10^{-3}. The relaxed stress is equal approximately to 120 MPa. The time interval t_{ni+1}-t_{ni} between neighbor points of the nth cycle of the stress relaxation curves varies from 0.01 to 0.05 s. The time to rupture t_r was calculated for the average stress in the time interval using P_{LM}. The parameter P_{LM} was determined from 63 creep rupture tests performed in the stress interval 80-480 MPa in the temperature range 730-1000 °C. The resulting times to fracture were in the interval 38.75 to 15335 hours [13].

The creep life fraction vs. number of cycles to fracture N_f is shown in Fig. 6 for the fatigue tests with hold-times. It is apparent that the creep damage represents only a few percents for all creep-fatigue tests. The fatigue damage, the first term in Eq. 4, is also low with the exception of high strain amplitudes – see Fig. 6. Therefore, the time-dependent-interaction damage D(tdi) (see Fig. 6) increases with increasing number of cycles to fracture. This behavior together with poor corrosion resistance of IN 713LC [2] suggests that environmental interactions represent a major part of the time-dependent-interaction damage. There is a scatter in experimental data caused primarily by the scatter in the size of the casting defects which reduce the fatigue life.

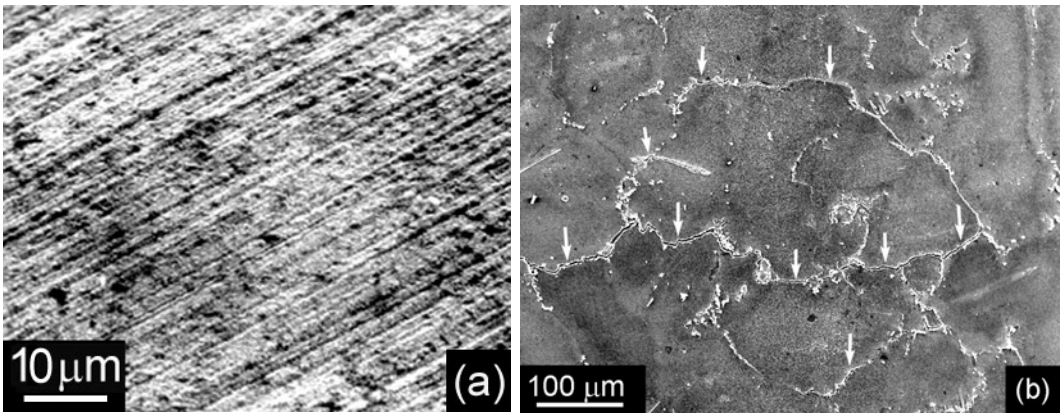

Fig. 7. SEM micrographs of surface relief. (a) Continuous cycling, ε_a = 0.8 %, (b) cycling with 10 min hold period, ε_a = 0.55 %.

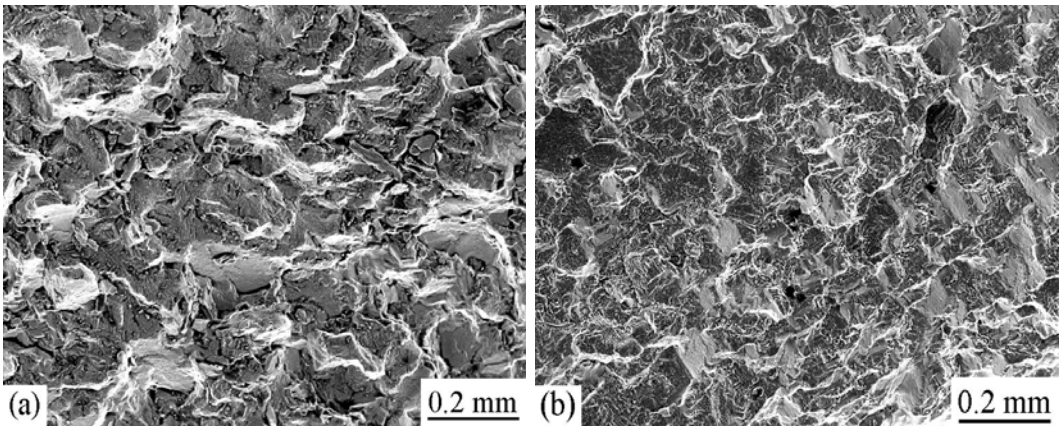

Fig. 8. Fracture surface in a distance of 0.5 mm from the specimen surface. (a) continuous cycling, ε_{ap} = 0.013 %, (b) cycling with 10 min dwell, ε_{ap} = 0.013 %.

3.3 Surface relief and fracture surface observation

Surface relief of specimens cycled with high strain amplitude to fracture in both types of tests is shown in Fig. 7. Figure 7a shows a SEM micrograph of the surface of a specimen cycled in continuous cycling. Inhomogeneous deformation resulting in high density of slip lines is apparent on a specimen fatigued in continuous cycling. Slip markings lie exclusively parallel to the {111} slip plane traces. Slip markings were not observed in all grains even in specimens cycled with very high strain amplitude. Fig. 7b shows the surface relief of a specimen fatigued with 10 min dwell. Numerous cracks (indicated with white arrows in Fig. 7b) initiated at dendritic grain boundaries are present. Cracks are observed also in interdendritic areas between individual dendritic arms. Besides, many carbides are visible at grain boundaries but some are apparent also inside the grains. However, slip markings were not observed on the surface of specimens

cycled with dwell to fracture. It can be concluded that the introduction of the 10 min dwell suppresses the formation of extrusions and intrusions.
Figure 8 shows SEM micrographs of the fracture surface of specimens cycled with two equal plastic strain amplitudes one in continuous cycling and second with 10 min dwell. Both fracture surfaces are in the same distance of 0.5 mm from the specimen surface. They are characterized by ductile fracture with a small number of facets. Striation areas, not shown in Fig 8, are present on fracture surfaces of both types of tests but much more often in continuous cycling. This is in agreement with existing findings that introduction of dwell periods in fatigue results in a shift from transgranular to intergranular mode of fracture [3,9].

SEM observation of sections parallel to the loading axis revealed that fatigue cracks initiate at grain boundaries but transgranular crack initiation along slip planes was also observed in continuous cycling. However, defects in the material present close to the surface accelerate the crack initiation and incipient crack growth.

Present results show that the introduction of the 10 min dwells reduces the fatigue life and influences damage mechanisms in IN 713LC particularly at an early stage of the lifetime. Important sources for these changes can be linked to fatigue-creep-environment interactions. Additional experimental data are needed to separate the role of the fatigue-creep interaction and environmentally assisted degradation.

4. Conclusions

(i) Fatigue life curves are dwell sensitive. For the given total strain amplitude, plastic strain amplitude and stress amplitude the fatigue life with dwells is reduced.

(ii) Damage analysis based on the Manson-Coffin curve and Larson-Miller parameter indicates the important role of fatigue-creep-environment interactions in life reduction due to hold periods.

(iii) Introduction of the 10 min dwell suppresses the formation of slip markings with extrusions and intrusions and modifies the crack initiation site and early crack propagation path.

Acknowledgements

This research was supported by the Grant Agency of the Czech Republic under grants No. 106/07/1507 and No. 106/08/1631 and by the grant No. 1QS200410502 of the Academy of Sciences of the Czech Republic.

References

[1] M.J. Donachie, S.J. Donachie, Superalloys: A Technical Guide, 2nd ed. ASM International, Materials Park, 2002, p. 260
[2] M.R. Winstone, Microstructure and alloy developments in nickel-based superalloys, in: A. Strang (Ed.), Microstructure of High Temperature Materials, Book 682, IOM Communications Ltd, London 1998, pp. 27-47
[3] P. Rodriguez S.L. Mannan, High temperature low cycle fatigue, Sadhana 20 (1995) 123-164
[4] T. Goswami: Low cycle fatigue – dwell effects and damage mechanisms, Int J Fatigue 21 (1999) 55-76
[5] L. Kunz, P. Lukáš, R. Mintách, R. Konečná, High-cycle fatigue of IN 713LC, in: J. Pokluda, P. Lukáš, P. Šandera, I. Dlouhý (Eds.), Proc. 17th Conference on Fracture, ESIS Czech Chapter, Brno 2008, CD, paper No. 101
[6] L. Kunz, P. Lukáš, R. Mintách, K. Hrbáček, Effect of mean stress on high-cycle fatigue strength of IN 713LC superalloy, Metall Mater 44 (2006) 275-281
[7] M. Petrenec, K. Obrtlík, J. Polák, Inhomogeneous dislocation structure in fatigued IN 713LC superalloy at room and elevated temperatures, Mater Sci Eng A 400-401 (2005) 485-488
[8] C.M. Sonsino, U. Brandt, J. Bergmann, Fatigue and short crack propagation behavior of cast nickel base alloys IN 713 C and Mar-M-247 LC at high temperature, in: K.-T. Rie (Ed.), Low Cycle Fatigue and Elasto-Plastic Behavior of Materials, Elsevier Science Ltd, London, 1992, pp. 262-268
[9] J. Polák, Cyclic Plasticity and Low Cycle Fatigue Life of Metals, Academia, Prague, 1991
[10] B. Fournier, M. Sauzay, C. Caës, M. Noblecourt, M. Mottot, A. Bourgault, V. Rabeau, J. Man, O. Gillia, P. Lomoine, A. Pineau, Creep-fatigue-oxidation interactions in a 9Cr-1Mo martensitic steel. Part III : Lifetime prediction, Int J Fatigue 30 (2008) 1797-1812
[11] J. Granacher, A. Scholz, Creep-fatigue behavior of heat resistant steels under service-type long-term conditions, in: K.-T. Rie (Ed.), Low Cycle Fatigue and Elasto-Plastic Behavior of Materials, Elsevier Science Ltd, London, 1992, pp. 235-241
[12] K. Obrtlík, J. Man, M. Petrenec, J. Polák, Room and high temperature low cycle fatigue of INCONEL 713 LC, in: EUROMAT 2001, Associazione Italiana di Metallurgia, Rimini 2001. CD, paper No. 894
[13] J. Hakl, T. Vlasák, High temperature properties of selected Ni base superalloys, Slévárenství 54 (2006) 444-452 (in Czech)